Journal of Materials Chemistry A

ROYAL SOCIETY OF CHEMISTRY

COMMUNICATION

View Article Online
View Journal | View Issue

Cite this: J. Mater. Chem. A, 2021, 9, 26676

Received 27th September 2021
Accepted 17th November 2021

DOI: 10.1039/d1ta08372d

rsc.li/materials-a

A high-throughput, solvent free method for dispersing metal atoms directly onto supports†

Emerson C. Kohlrausch,[ab] Higor Andrade Centurion,[c] Rhys W. Lodge,[a] Xuanli Luo,[d] Thomas Slater,[e] Marcos J. L. Santos,[b] Sanliang Ling,[d] Valmor R. Mastelaro,[c] Matthew J. Cliffe,[a] Renato Vitalino Goncalves[c] and Jesum Alves Fernandes*[a]

Atomically-dispersed metal catalysts (ADMCs) on surfaces have demonstrated high activity and selectivity in many catalytic reactions. However, dispersing and stabilising individual atoms in support materials in an atom/energy-efficient scalable way still presents a significant challenge. Currently, the synthesis of ADMCs involves many steps and further filtration procedures, creating a substantial hurdle to their production at industrial scale. In this work, we develop a new pathway for producing ADMCs in which Pt atoms are stabilised in the nitrogen-interstices of a graphitic carbon nitride (g-C_3N_4) framework using scalable, solvent-free, one-pot magnetron sputtering deposition. Our approach has the highest reported rate of ADMC production of 4.8 mg h^{-1} and generates no chemical waste. Deposition of only 0.5 weight percent of Pt onto g-C_3N_4 led to improved hydrogen production by factor of *ca.* 3333 ± 450 when compared to bare g-C_3N_4. PL analysis showed that the deposition of Pt atoms onto g-C_3N_4 suppressed the charge carrier recombination from the photogenerated electron–hole pairs of Pt/g-C_3N_4 thereby enhance hydrogen evolution. Scanning transmission electron microscope imaging before and after the hydrogen evolution reaction revealed that the Pt atoms stabilised in g-C_3N_4 have a high stability, with no agglomeration observed. Herein, it is shown that this scalable and clean approach can produce effective ADMCs with no further synthetic steps required, and that they can be readily used for catalytic reactions.

Introduction

Atomically-dispersed metal catalysts (ADMCs) bridge the gap between homogenous and heterogeneous catalysis[1–3] and can combine the best features of both: the high activity and selectivity of homogenous catalysts with the high stability and recyclability of heterogeneous catalysts.[4–6] Current methods for the synthesis of ADMCs are based on either wet-chemistry (*i.e.* reduction of metal salts) or atomic layer deposition (ALD).[6–12] However, industrial scale-up of these synthetic methods is difficult because they require multiple steps and/or high temperatures, generate large amounts of chemical waste, and are not readily generalisable across supports and metal catalysts. In contrast, top-down physical methods[7,13–15] for ADMC synthesis do not need high-temperatures and can be used for almost any type of solid support and transition metals without generating chemical waste. However, most physical methods are intrinsically limited to making small quantities of materials, and therefore are not scalable to industrial levels.[16]

Magnetron sputtering has recently emerged as a promising technique for the production of metal nanoparticles (MNPs) on a wide variety of supports (*e.g.* powder, liquids).[17–22] It is one of the select few 'green' and scalable top-down methods,[17] and has already been applied on a large scale in the glass-coating and semiconductor industries. Crucially, this approach is carried out in ultraclean, high vacuum environments and can therefore generate extremely active metal species with clean surfaces not occluded by ligands or surfactants.[17,18,23] In the magnetron sputtering process, accelerated argon (Ar) ions collide elastically with a highly pure metal target, which expels atoms onto a support material (Fig. 1a). Gohara & Yamazaki recently demonstrated that single Pt atoms can be dispersed and stabilised onto a single layer graphene deposited onto TEM grids using magnetron sputtering deposition.[24] However, the deposition of ADMCs into bulk powder samples, suitable for use at scale and thus in catalysis, has not been demonstrated.

Herein we show, for the first time, the deposition of ADMCs into bulk powder using magnetron sputtering. We stabilised Pt atoms into the nitrogen-interstices of graphitic carbon nitride (g-

[a]School of Chemistry, University of Nottingham, Nottingham, NG7 2RD, UK. E-mail: jesum.alvesfernandes@nottingham.ac.uk

[b]Programa de Pós-Graduação em Ciência dos Materiais, Universidade Federal do Rio Grande do Sul, Porto Alegre, RS, 91501-970, Brazil

[c]São Carlos Institute of Physics, University of São Paulo, São Carlos, SP, 13560-970, Brazil

[d]Advanced Materials Research Group, Faculty of Engineering, University of Nottingham, Nottingham, NG7 2RD, UK

[e]Electron Physical Sciences Imaging Centre, Diamond Light Source Ltd., Oxfordshire, OX11 0DE, UK

† Electronic supplementary information (ESI) available: Sample preparation process, experimental techniques, additional figures, tables, and references. See DOI: 10.1039/d1ta08372d

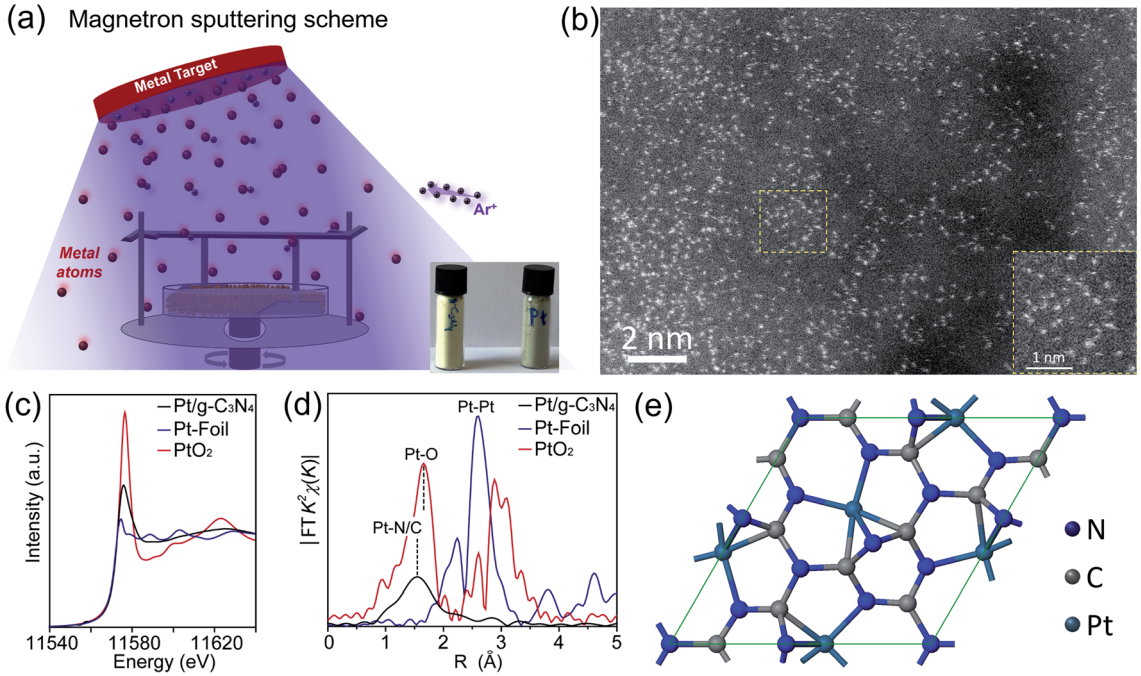

Fig. 1 (a) Schematic representation of Pt atom deposition onto g-C_3N_4 using magnetron sputtering (not to scale). (b) Aberration corrected-scanning transmission electron microscope (AC-STEM) image shows the high dispersion of Pt atoms in g-C_3N_4. (c and d) XANES and Fourier transformed EXAFS spectra of Pt/g-C_3N_4, Pt foil and PtO_2, respectively (e) DFT optimised structure of Pt atoms stabilised onto threefold nitrogen-interstice between *s*-triazine units in g-C_3N_4 framework.

C_3N_4). Furthermore, our approach showed the highest rate of ADMC production reported so far (at least 7.6 times higher than the previous benchmark[3,6,25]), and does so without generating chemical waste (Table S5†). The deposition and stabilisation of Pt atoms onto a g-C_3N_4 framework was confirmed by aberration corrected scanning transmission electron microscopy (AC-STEM) and extended X-ray absorption fine structure (EXAFS) measurements, and was further supported by density functional theory (DFT) calculations. Furthermore, the photocatalytic performance of Pt/g-C_3N_4 was tested for hydrogen evolution. Our Pt/g-C_3N_4 shows outstanding photocatalytic activity when compared with similar reported systems (Table S6†). AC-STEM and X-ray photoelectron spectroscopy (XPS) analysis before and after the hydrogen evolution reaction confirmed the stability of Pt atoms on a g-C_3N_4 framework. These results demonstrate that the scalable magnetron sputtering approach can generate effective ADMCs for catalytic processes such as hydrogen generation using only one clean synthetic step.

Results

g-C_3N_4 was prepared *via* pyrolysis of melamine (10 g), heating under air at 300 °C for 2 hours and then 520 °C for 2 hours (Scheme S1†).[26] The chemical composition and crystalline structure of the synthesised g-C_3N_4 support was confirmed by Fourier-transform infrared spectroscopy (FTIR), powder X-ray diffraction (PXRD) and XPS measurements (see the ESI† for details).

The deposition of Pt atoms on g-C_3N_4 *via* magnetron sputtering was carried out using a bespoke AJA International system (Fig. S1, see the ESI† for details). g-C_3N_4 (1 g) was placed into a tailor-made stirring sample-holder, and then loaded into the magnetron sputtering chamber (reaching 3×10^{-8} torr background pressure in 40 min). After waiting 10 min for background pressure stabilisation, Ar gas (99.9999%) was introduced into the chamber, reaching 3×10^{-3} torr. Upon using an applied power (370 V and 16 mA), highly energetic ions were accelerated against the Pt target leading to a cascade of collisions at the surface of the Pt target, thus ejecting primarily individual neutral Pt atoms from the target[22,27,28] which were then deposited onto the g-C_3N_4 framework (Fig. 1a). The g-C_3N_4 powder was stirred constantly during the Pt atoms deposition to allow for atomic dispersion throughout the whole powder (Fig. 1a). In this fashion, Pt atoms deposition was carried out for 12 min, yielding Pt/g-C_3N_4 (0.5 wt% of Pt onto 1 g of g-C_3N_4) measured by inductively coupled plasma optical emission spectrometry (ICP-OES). This gave an ADMC production-rate of 4.8 mg h^{-1}, with a Pt loading on g-C_3N_4 of 5 mg and a total 'feedstock-to-product' magnetron sputtering process time of 63 min, which is the highest rate of production reported so far (Table S5†). Diverse characterisation techniques revealed no significant differences after deposition of the Pt atoms onto g-C_3N_4, including FTIR, PXRD, specific surface area and CHN elemental analysis (Fig. S2, S3 and Table S1†). Notably, the PXRD data show no evidence of either Pt or PtO_2 in bulk or nanoparticulate form (Fig. S2b†). To demonstrate the generality of this method, Ni and Co atoms were atomically dispersed onto g-C_3N_4 framework using similar parameters (Fig. S5†).

AC-STEM measurements revealed highly dispersed Pt atoms in the g-C_3N_4 framework, with no Pt NPs observed (Fig. 1b and S3†). XAS measurements were performed to probe the local environment of Pt atoms (Fig. 1c and d). Fig. 1c shows the

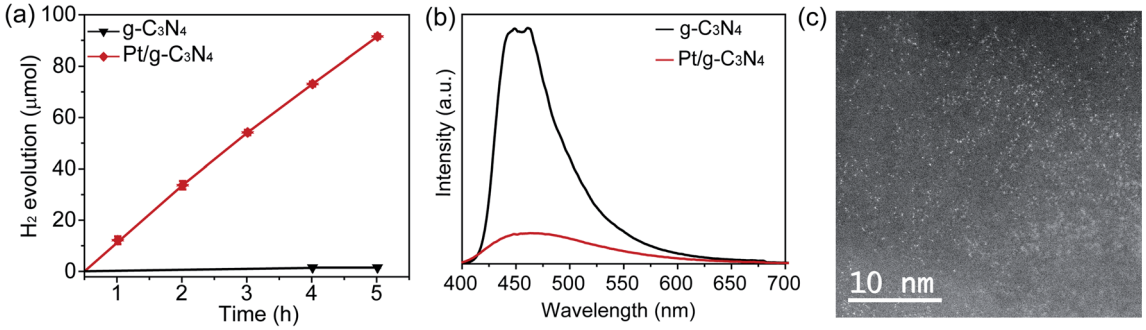

Fig. 2 (a) Photocatalytic hydrogen production using 1 mg ml^{-1} of photocatalyst, 10 vol% of TEOA, irradiation intensity of 300 mW cm^{-2}, filter AM 1.5 G, at 30 °C. (b) Photoluminescence spectra of g-C_3N_4 and Pt/g-C_3N_4 (excitation at 350 nm). (c) AC-STEM image shows that the high dispersion of Pt atoms on g-C_3N_4 is retained after the reaction.

XANES spectrum of Pt/g-C_3N_4, and the standard spectra of Pt foil and PtO_2. The white line intensities of these spectra revealed the oxidation state of the Pt atoms in each case, and the intensity for Pt/g-C_3N_4 was intermediate between that of Pt foil and PtO_2. This suggested that Pt atoms were slightly positively charged due to coordination with the g-C_3N_4 framework, which agreed with XPS measurements (Fig. S3a†).[29–31] The Pt K-edge EXAFS of Pt/g-C_3N_4 showed only one peak at *ca.* 1.5 Å (not phase-corrected), which can be associated to Pt–N/C coordination (Fig. 1d and Table S2†).[10,30,31] No peaks associated with Pt–Pt and/or Pt–O coordination were observed (Fig. 1d), which is consistent with the AC-STEM and PXRD analysis. To obtain further atomistic insight into the interaction between Pt atoms and g-C_3N_4, DFT calculations were performed (see the ESI† for details). For these calculations, the nitrogen-interstice of *s*-triazine and tri-*s*-triazine units of g-C_3N_4 framework were considered as sites for stabilisation of single Pt atoms (Fig. S6 and Table S3†).[32] Therefore, we suggest that Pt atoms were stabilised in the threefold nitrogen-interstice (Fig. 1e), as the first EXAFS peak appeared at a slightly shorter bond distance than would be expected for Pt–O, whereas the sixfold nitrogen Pt–N appeared at a slightly longer bond distance than Pt–O (Tables S2 and S3†). This corroborated with our EXAFS results and previous reports on Pt atoms stabilisation onto g-C_3N_4.[10,31]

Photocatalytic hydrogen production reactions were performed to investigate the catalytic photoactivity of Pt/g-C_3N_4 and g-C_3N_4 (Fig. 2a and Table S4†). As expected, pristine g-C_3N_4 showed negligible hydrogen evolution and hydrogen was only detected in large enough quantities to be reliably measured after 3 h. In contrast, Pt/g-C_3N_4 showed a much higher activity, improving the hydrogen production 3333 ± 450 times after 5 h of reaction. Moreover, our results compare favourably to similar systems previously reported, demonstrating the high photocatalytic activity of our Pt/g-C_3N_4 system (Table S6†).

To gain further insights into the high photocatalytic activity of Pt/g-C_3N_4, we carried out photoluminescence (PL) measurements to investigate the efficiency of charge transfer and separation (Fig. 2b). The PL spectrum of g-C_3N_4 exhibits an intense peak at *ca.* 460 nm, which is ascribed to electron–hole recombination of g-C_3N_4. The deposition of Pt onto the g-C_3N_4 surface led to a decrease of the PL intensity, implying suppressed charge carrier recombination (Fig. 2b) arising from the efficient dissociation of photogenerated electron–hole pairs of Pt/g-C_3N_4, in agreement with the photocatalytic results.[33,34] AC-STEM images and XPS analysis of the Pt/g-C_3N_4 after 5 h under reactions conditions show no agglomeration and no significantly changes in Pt electronic properties (Fig. 2c and S7,† respectively), the major mechanism responsible for catalyst deactivation, which demonstrates the high stability of Pt atoms in the g-C_3N_4 framework.

Conclusion

In summary, we have demonstrated a new approach for producing ADMCs, using magnetron sputtering to deposit Pt atoms into a g-C_3N_4 support. This approach has the highest reported rate of ADMC production out of all preparation routes. The Pt/g-C_3N_4 photocatalyst generated using this approach is very effective for photocatalytic hydrogen production, which is attributed to the synergy between Pt atoms and g-C_3N_4. Our results suggest that Pt atoms were stabilised in the nitrogen-interstices of the g-C_3N_4 framework. AC-STEM analysis after hydrogen evolution reaction revealed the high stability of Pt atoms in g-C_3N_4. This approach is readily generalisable to other metals (*i.e.* Ni and Co), raising the possibility of straightforward and scalable synthesis of a wide range of ADMCs. As a result, we believe this strategy could therefore be a transformative method for the synthesis of ADMCs, potentially changing how to synthetise ADMCs at both the research and industrial scales.

Author contributions

E. C. K. designed the experiments and performed the synthesis and characterisation of g-C_3N_4, and magnetron sputtering depositions. R. W. L. and T. S. carried out TEM and AC-STEM measurements and analysis. H. A. C. and R. V. G. conducted photocatalytic experiments. S. L. performed DFT calculations. V. R. M. and X. L. carried out XANES and EXAFS measurements and analysis. M. J. L. S., M. J. C., R. V. G. and J. A. F. designed the study, supervised the project and co-wrote the paper. All the authors discussed the results and commented on the manuscript.

Conflicts of interest

The authors declare no competing financial interest.

Acknowledgements

The authors thank the University of Nottingham Propulsion Futures and Green Chemicals Beacons of Excellence, and Hobday Fund for the financial support, the Nanoscale and Microscale Research Centre (nmRC) for access to materials characterisation equipment. The authors acknowledge support of EPSRC Metal Atoms on Surfaces and Interfaces (MASI) for Sustainable Future programme grant (EP/V000055/1) for the financial support. We thank the use of the Athena supercomputer through the HPC Midlands+ Consortium, and the ARCHER2 supercomputer through membership of the UK's HPC Materials Chemistry Consortium, which are funded by EPSRC [grant number EP/P020232/1] and [grant number EP/R029431/1], respectively. We also thank the São Paulo Research Foundation (FAPESP, Grant 2017/18716-3, 2013/07296-2), CNPq, CAPES for financial support. Thanks to Alan Chadwick and Giannantonio Cibin for the XAS measurements, and Diamond Light Source for provision of beam time through the Block Allocation Group (BAG) for Energy Materials under proposal sp17198 B18 BAG and to the electron Physical Sciences Imaging Centre (ePSIC instrument E01 under proposal MG24914); and to MAX IV Laboratory for provision of beam time under proposal p20190402.

References

1 A. Wang, J. Li and T. Zhang, *Nat. Rev. Chem.*, 2018, **2**, 65–81.
2 A. J. Therrien, A. J. R. Hensley, M. D. Marcinkowski, R. Zhang, F. R. Lucci, B. Coughlin, A. C. Schilling, J.-S. McEwen and E. C. H. Sykes, *Nat. Catal.*, 2018, **1**, 192–198.
3 M. Liu, L. Wang, K. Zhao, S. Shi, Q. Shao, L. Zhang, X. Sun, Y. Zhao and J. Zhang, *Energy Environ. Sci.*, 2019, **12**, 2890–2923.
4 Y. Peng, Z. Geng, S. Zhao, L. Wang, H. Li, X. Wang, X. Zheng, J. Zhu, Z. Li, R. Si and J. Zeng, *Nano Lett.*, 2018, **18**, 3785–3791.
5 Y. Chen, S. Ji, C. Chen, Q. Peng, D. Wang and Y. Li, *Joule*, 2018, **2**, 1242–1264.
6 X. Sun, S. R. Dawson, T. E. Parmentier, G. Malta, T. E. Davies, Q. He, L. Lu, D. J. Morgan, N. Carthey, P. Johnston, S. A. Kondrat, S. J. Freakley, C. J. Kiely and G. J. Hutchings, *Nat. Chem.*, 2020, **12**, 560–567.
7 Z. Y. Li, N. P. Young, M. Di Vece, S. Palomba, R. E. Palmer, A. L. Bleloch, B. C. Curley, R. L. Johnston, J. Jiang and J. Yuan, *Nature*, 2008, **451**, 46–48.
8 H. Yan, Y. Lin, H. Wu, W. Zhang, Z. Sun, H. Cheng, W. Liu, C. Wang, J. Li, X. Huang, T. Yao, J. Yang, S. Wei and J. Lu, *Nat. Commun.*, 2017, **8**, 1070.
9 X. Guo, G. Fang, G. Li, H. Ma, H. Fan, L. Yu, C. Ma, X. Wu, D. Deng, M. Wei, D. Tan, R. Si, S. Zhang, J. Li, L. Sun, Z. Tang, X. Pan and X. Bao, *Science*, 2014, **344**, 616.
10 X. Li, W. Bi, L. Zhang, S. Tao, W. Chu, Q. Zhang, Y. Luo, C. Wu and Y. Xie, *Adv. Mater.*, 2016, **28**, 2427–2431.
11 X. Fang, Q. Shang, Y. Wang, L. Jiao, T. Yao, Y. Li, Q. Zhang, Y. Luo and H.-L. Jiang, *Adv. Mater.*, 2018, **30**, 1705112.
12 H. Xiang, W. Feng and Y. Chen, *Adv. Mater.*, 2020, **32**, 1905994.
13 S. Abbet, A. Sanchez, U. Heiz, W. D. Schneider, A. M. Ferrari, G. Pacchioni and N. Rösch, *J. Am. Chem. Soc.*, 2000, **122**, 3453–3457.
14 R. Balavinayagam, M. Somik, J. M. Cherian, G. Keshab and G. Shubhra, *Nanotechnology*, 2013, **24**, 205602.
15 R. E. Palmer, R. Cai and J. Vernieres, *Acc. Chem. Res.*, 2018, **51**, 2296–2304.
16 H. Yan, C. Su, J. He and W. Chen, *J. Mater. Chem. A*, 2018, **6**, 8793–8814.
17 Y. Ishida, R. D. Corpuz and T. Yonezawa, *Acc. Chem. Res.*, 2017, **50**, 2986–2995.
18 L. Luza, C. P. Rambor, A. Gual, J. Alves Fernandes, D. Eberhardt and J. Dupont, *ACS Catal.*, 2017, **7**, 2791–2799.
19 T. Torimoto, K.-i. Okazaki, T. Kiyama, K. Hirahara, N. Tanaka and S. Kuwabata, *Appl. Phys. Lett.*, 2006, **89**, 243117.
20 R. V. Gonçalves, R. Wojcieszak, H. Wender, C. S. B. Dias, L. L. R. Vono, D. Eberhardt, S. R. Teixeira and L. M. Rossi, *ACS Appl. Mater. Interfaces*, 2015, **7**, 7987–7994.
21 R. V. Gonçalves, H. Wender, P. Migowski, A. F. Feil, D. Eberhardt, J. Boita, S. Khan, G. Machado, J. Dupont and S. R. Teixeira, *J. Phys. Chem. C*, 2017, **121**, 5855–5863.
22 I. Cano, A. Weilhard, C. Martin, J. Pinto, R. W. Lodge, A. R. Santos, G. A. Rance, E. H. Åhlgren, E. Jónsson, J. Yuan, Z. Y. Li, P. Licence, A. N. Khlobystov and J. Alves Fernandes, *Nat. Commun.*, 2021, **12**, 4965.
23 L. Calabria, J. A. Fernandes, P. Migowski, F. Bernardi, D. L. Baptista, R. Leal, T. Grehl and J. Dupont, *Nanoscale*, 2017, **9**, 18753–18758.
24 K. Yamazaki, Y. Maehara, C.-C. Lee, J. Yoshinobu, T. Ozaki and K. Gohara, *J. Phys. Chem. C*, 2018, **122**, 27292–27300.
25 L. Liu, S. Liu, L. Li, H. Qi, H. Yang, Y. Huang, Z. Wei, L. Li, J. Xu and B. Liu, *J. Mater. Chem. A*, 2020, **8**, 6190–6195.
26 Z. Mo, X. She, Y. Li, L. Liu, L. Huang, Z. Chen, Q. Zhang, H. Xu and H. Li, *RSC Adv.*, 2015, **5**, 101552–101562.
27 I. Petrov, A. Myers, J. E. Greene and J. R. Abelson, *J. Vac. Sci. Technol., A*, 1994, **12**, 2846–2854.
28 K. Macák, V. Kouznetsov, J. Schneider, U. Helmersson and I. Petrov, *J. Vac. Sci. Technol., A*, 2000, **18**, 1533–1537.
29 B. Qiao, A. Wang, X. Yang, L. F. Allard, Z. Jiang, Y. Cui, J. Liu, J. Li and T. Zhang, *Nat. Chem.*, 2011, **3**, 634–641.
30 H. Shin, W.-G. Jung, D.-H. Kim, J.-S. Jang, Y. H. Kim, W.-T. Koo, J. Bae, C. Park, S.-H. Cho, B. J. Kim and I.-D. Kim, *ACS Nano*, 2020, **14**, 11394–11405.
31 Z. Zeng, Y. Su, X. Quan, W. Choi, G. Zhang, N. Liu, B. Kim, S. Chen, H. Yu and S. Zhang, *Nano Energy*, 2020, **69**, 104409.
32 C. Rivera-Cárcamo and P. Serp, *ChemCatChem*, 2018, **10**, 5058–5091.
33 J. Yang, D. Wang, H. Han and C. Li, *Acc. Chem. Res.*, 2013, **46**, 1900–1909.
34 K. Li, Z. Zeng, L. Yan, S. Luo, X. Luo, M. Huo and Y. Guo, *Appl. Catal., B*, 2015, **165**, 428–437.